Planta (2011) 234:21–34
DOI 10.1007/s00425-011-1372-5

ORIGINAL ARTICLE

The fatal effect of tungsten on *Pisum sativum* L. root cells: indications for endoplasmic reticulum stress-induced programmed cell death

Ioannis-Dimosthenis S. Adamakis · Emmanuel Panteris · Eleftherios P. Eleftheriou

Received: 22 December 2010 / Accepted: 25 January 2011 / Published online: 23 February 2011

Abstract Programmed cell death (PCD) is a widespread response of plants against abiotic stress, such as heavy metal toxicity. Tungsten (W) is increasingly considered toxic for plants since it irreversibly affects their growth. Therefore, we investigated whether W could induce some kind of PCD in plants, like other heavy metals do. The morphology of cell and nucleus, the integrity of the cytoskeleton, Evans Blue absorbance and the expression of PCD-related genes were used as indicators of PCD in W-treated roots of *Pisum sativum* (pea). TEM and fluorescence microscopy revealed mitotic cycle arrest, protoplast shrinkage, disruption of the cytoskeleton and chromatin condensation and peripheral distribution in the nucleus of W-affected cells. Moreover, Evans Blue absorbance in roots increased in relation to the duration of W treatment. These effects were suppressed by inhibitors of the 26S proteasome, caspases and endoplasmic reticulum stress. In addition, silencing of *DAD-1* and induction of *HSR203J*, *BiP-D*, *bZIP28* and *bZIP60* genes were also recorded in W-treated pea roots by semi-quantitative RT-PCR. The above observations show that W induces a kind of PCD in pea roots, further substantiating its toxicity for plants. Data imply that endoplasmic reticulum stress-unfolded protein response may be involved in W-induced PCD.

Keywords 26S proteasome · Caspase-like proteases · Endoplasmic reticulum stress (ER stress) · Microtubules · Programmed cell death (PCD) · Tungsten (W) · Unfolded protein response (UPR)

Abbreviations

ER	Endoplasmic reticulum
ERAD	ER associated degradation
PCD	Programmed cell death
PBA	4-Phenylbutyric acid
UPR	Unfolded protein response

Introduction

Several metals have been proven to be toxic for plants. One of the responses of plants to such toxicity is the execution of programmed cell death (PCD). For example, this was shown for cadmium (Iakimova et al. 2008; Kuthanova et al. 2008) and aluminium (Pan et al. 2001; Tamas et al. 2005). Tungsten (W) is a scarce heavy metal in nature, but it is locally accumulated at high concentrations as a waste of mines, industries, agricultural and military activities (Wilson and Pyatt 2006; Clausen and Korte 2009 and references therein). Over the last decade, W has attracted the attention of scientists, since it was shown to be toxic for living organisms (Koutsospyros et al. 2006; Steinberg et al. 2007). In particular, Koutsospyros et al. (2006) stated: "…it appears that environmental obscurity for tungsten and its compounds has ended and environmental scrutiny has emerged".

Tungsten toxicity in plants has been initially related to the competition with its chemical relative, molybdenum (Mo), since it binds to molybdoenzymes and inactivates

Electronic supplementary material The online version of this article (doi:10.1007/s00425-011-1372-5) contains supplementary material, which is available to authorized users.

I.-D. S. Adamakis (✉) · E. Panteris (✉) · E. P. Eleftheriou
Department of Botany, School of Biology, Aristotle University of Thessaloniki, 541 24 Thessaloniki, Macedonia, Greece
e-mail: iadamaki@bio.auth.gr

E. Panteris
e-mail: epanter@bio.auth.gr

them (for references see Adamakis et al. 2010a). Further toxic effects of W in plants have been reported. Pea (*Pisum sativum*) and cotton (*Gossypium hirsutum*) seedlings grown in the presence of W showed specific defects in the root system: primary root elongation was irreversibly arrested, meristematic root cells were prematurely vacuolated and the morphology of the nucleus and nucleolus was altered (Adamakis et al. 2008). Moreover, it was recently described that W severely affected the cortical microtubules (Adamakis et al. 2010a, b). Interestingly, disruption of the cytoskeleton is one of the primary features of certain types of plant PCD (Pontier et al. 2004). For instance, microtubule disorganization occurs in self-incompatibility-mediated PCD of *Papaver rhoeas* pollen (Bosch et al. 2008; Poulter et al. 2008). Recently, it has been reported that exposure to W is correlated with apoptosis in human blood lymphocytes (Osterburg et al. 2010). Taking into account these data from pea, as well as the above report from human cells, we examined the possibility that W toxicity to pea roots may be associated with some type of PCD.

Plant PCD involves several structural and biochemical/molecular features (Reape et al. 2008). In this study, the appearance of cortical microtubules in W-treated pea roots was used as a PCD indicator, in addition to Evans Blue staining and protoplast shrinkage. The expression of PCD-related genes, *DAD-1* (*d*efender against *a*poptotic cell *d*eath-1, Orzáez and Granell 1997; Tanaka et al. 1997) and *HSR203J* (involved in hypersensitive response, Pontier et al. 1998; Bézier et al. 2002; Pontier et al. 2004) was also examined. In parallel, the participation of the pathways of the 26S proteasome and the caspase-like plant enzymes (among others see Bosch and Franklin-Tong 2007; Bonneau et al. 2008) were indirectly investigated. Our findings indicate that W toxicity seems to be associated with some kind of PCD. The expression profiles of three relevant genes (*BiP-D, bZIP28* and *bZIP60*) also suggest that endoplasmic reticulum (ER) stress-unfolded protein response (UPR) is probably involved.

Materials and methods

Plant material, treatments with W and inhibitors

Intact 4- to 5-day-old *Pisum sativum* L. cv. Onmard (pea) (Spyrou Company, Athens, Greece) seedlings, grown on wet filter paper in the dark at 25°C, were used in all procedures. Chemicals, reagents, stains and antibodies, except those stated, were purchased from Sigma-Aldrich (Taufkirchen, Germany) and Merck (Darmstadt, Germany). All experimental procedures were carried out at room temperature, unless otherwise stated. Some seedlings were treated for 12–72 h with an aqueous 200 mg/L sodium tungstate (Na_2WO_4) solution (1 μM), pH 5.7 (Adamakis et al. 2008). This concentration was used taking into account the fact that in some cases of W pollution, its concentration was found to vary between 135 and 337 mg/L (review by Koutsospyros et al. 2006). For control, seedlings of the same age were treated at the same time with a buffer pH 5.7.

The 26S proteasome inhibitor Z-Leu-Leu-Leu-al (MG132) and the pan-caspase inhibitor Z-Val-Ala-Asp(OMe)-CH_2F (Z-VAD-FMK, Calbiochem, Darmstadt, Germany) were used for inhibition of the respective protease pathways. Stock solutions of both inhibitors (100 and 50 mM, respectively) were prepared in dimethyl sulfoxide (DMSO). Seedlings pre-treated for 24 h with 100 μM MG132 were transferred to a 200 mg/L W + 100 μM MG132 solution for another 24 h. Some seedlings were treated directly with a 200 mg/L W + 100 μM MG132 solution for 24 h. For control, seedlings treated with 100 μM MG132 for 24 h were used. Some seedlings were pre-treated for 24 h with 100 μM Z-VAD-FMK and afterwards with a 200 mg/L W + 100 μM Z-VAD-FMK solution for 24 h more. In some other seedlings a 200 mg/L W + 100 μM Z-VAD-FMK solution was directly applied for 24 h. Seedlings treated with 100 μM Z-VAD-FMK were considered as controls.

4-Phenylbutyric acid (PBA), a chemical suppressor of ER stress (Wiley et al. 2010 and references therein), was used to indirectly check whether W-induced PCD is ER stress mediated. Seedlings were treated directly with an aqueous 200 mg/L W + 250 μM PBA solution for 24 h. For control, seedlings treated with aqueous 250 μM PBA were used.

Tubulin immunostaining, DNA and F-actin staining and fluorescence microscopy

Root tips from seedlings treated as described above were prepared for tubulin immunofluorescence, DNA and F-actin fluorescence. For tubulin immunostaining and DNA staining, root tips were cut and fixed for 45 min in 8% (w/v) paraformaldehyde in PEM buffer (50 mM PIPES, 5 mM EGTA, 5 mM $MgSO_4$, pH 6.8; Adamakis et al. 2010a). After washing in PEM, the cell walls were digested, then the root tips were gently squashed onto polylysine-coated coverslips and when the separated cells dried, they were extracted for 1 h. The cells were then incubated overnight with rat anti-α-tubulin antibody (YOL 1/34, Serotec, Kidlington, UK) diluted 1:80 in PEM. Following washing with PEM, the cells were incubated overnight with FITC-anti-rat 1:80 in the same buffer. DNA was counterstained with 3 μg/mL propidium iodide in PEM and the coverslips were finally mounted in an anti-fade solution.

F-actin staining of root tips was carried out according to Panteris et al. (2007). In short, hand cut longitudinal sheets of root tips were incubated with 300 μM *m*-maleimidobenzoyl-*N*-hydroxysuccinimide ester (MBS) in PEM buffer, pH 6.8, plus 0.1% (v/v) Triton X-100 and 2% (v/v) DMSO, for 30 min in the dark, to stabilize F-actin. After stabilization, fixation was performed in 4% (w/v) paraformaldehyde (PFA) in the same buffer for 60 min. In the fixative solution 1% (v/v; diluted from a stock 10 μM solution in methanol) TRITC-phalloidin was added. The tissue sheets were then rinsed with PEM and extracted in 5% (v/v) DMSO with 1% (v/v) Triton X-100 in the same buffer, for 1 h. Finally, actin filaments were stained with 10% (v/v; same as before) TRITC-phalloidin in PEM overnight in the dark. All fluorescent specimens were examined with a Nikon D-Eclipse C1 confocal laser scanning microscope (CLSM).

Transmission electron microscopy (TEM)

For TEM, root tips (2 mm long) were excised and fixed for 5 h in 2% paraformaldehyde + 3% glutaraldehyde, in 0.05 M sodium cacodylate buffer, pH 7.0 (Adamakis et al. 2008). The samples were then post-fixed in 2% osmium tetroxide (Agar Scientific, Essex, UK) in the same buffer for 5 h, dehydrated in an acetone series, treated with propylene oxide, embedded in Durcupan ACM resin (Fluka Chemie AG, Buchs, Switzerland) and sectioned with a Reichert–Jung Ultracut E ultramicrotome. Ultrathin sections (80–90 nm) were double-stained with 2% uranyl acetate and 1% lead citrate and examined with a Zeiss 9 S-2 electron microscope.

Evans Blue and FM4-64 staining

Evans Blue staining was done following the protocol by Chen et al. (2008). In short, ten roots were randomly selected from seedlings subjected to various treatments. The roots were incubated in a 0.25% aqueous Evans Blue solution for 15 min at room temperature. The roots were then washed twice with double-distilled water and left in distilled water overnight. The apical 5 mm part of the root tips was excised and the dye was extracted in an aqueous solution of 50% methanol/1% SDS for 1 h at 50°C. Optical density (OD) of extracts was measured at 595 nm with a spectrophotometer (UV-2401PC, Shimadzu, Kyoto, Japan or SmartSpec Plus, Biorad, Herts, UK). Data are presented as mean ± standard error (SE) of three independent experiments. Statistical analyses (ANOVA with Dunnett's multiple comparison test) were performed using Graph Pad Prism (Graph Pad Software, San Diego, CA, USA) with significance at $P < 0.05$.

Whole roots of seedlings treated with W for 24 h, as well as of untreated ones were immersed for 10 min in an aqueous 5 μM FM4-64 solution (Invitrogen, Carlsbad, CA, USA; diluted from a 10 mM stock solution in DMSO). Afterwards, the roots were thoroughly washed with double-distilled water and their tips, 2 to 3 mm long, were cut, placed on microscope slides and observed with CLSM.

DNA and RNA isolation and gene expression

Total DNA from roots treated with 200 mg/L W for 12–72 h and RNA from roots treated with 200 mg/L W for 12–24 h, as well as from untreated ones, was isolated using the NucleoSpin Plant II and NucleoSpin RNA plant kits (Macherey–Nagel, Düren, Germany), respectively, following the manufacturer's instructions. First strand cDNA was synthesized from 2 μg total RNA in a volume of 20 μL with AMV-Reverse Transcriptase (Promega, Madison, WI, USA) according to the manufacturer's protocol. Levels of specific mRNA transcripts were assayed by PCR in a mixture of 50 μL, using DyNAzyme II DNA polymerase (Finnyzymes, Espoo, Finland). Gene-specific primers for *Pisum sativum DAD-1, HSR203J* homologs, the soybean *BiP-D* (Cascardo et al. 2000), *bZIP28* and *bZIP60* homologs (Liao et al. 2008) are listed in Table 1. *ACTIN* expression was used as control. To verify the exponential phase of PCR amplification, 20, 25 and 30 cycles were tested for each gene. The PCR products as well as total DNA were subject to 1 or 2% agarose gel electrophoresis and visualized by ethidium bromide staining. Furthermore, the expression profile of all the mentioned genes was also examined in root tips of seedlings subjected to: (a) a 24 h pre-treatment with 100 μM MG132 and afterwards a combined 24 h treatment with a 200 mg/L W + 100 μM MG132 solution, (b) 24 h pre-treatment with 100 μM Z-VAD-FMK and afterwards with a 200 mg/L W + 100 μM Z-VAD-FMK solution for 24 h more, and (c) a direct 24 h treatment with an aqueous 200 mg/L W + 250 μM PBA solution.

Results

Cell morphology and Evans Blue absorbance of W-affected pea roots

After 24–72 h of W treatment, root cells died, as confirmed by cell appearance and Evans Blue staining. Evans Blue absorbance was enhanced, as treatment time increased (Fig. 1). FM4-64 staining revealed that in many cells the protoplast was shrunk, retracting completely from the cell wall (Fig. 2b; cf. a). Because of the thickness and complexity of pea root as a whole organ, this observation was

Table 1 Primers used to amplify genes by RT-PCR

Gene	Forward primer	Reverse primer
HSR203 J	5′-TGTCCGGTTGGCTTAGAATC-3′	5′-GAGAAACGGGGAGACACAAA-3′
DAD-1	5′-CTATTCCACGCTATTTGGTC-3′	5′-ATGATCACCAAATGAAGCAC-3′
BiP-D	5′-ATCTGGAGGAGCCCTAGGCGGTGG-3′	5′-CTTGAAGAAGCTTCGTCGTAAAACTAAG-3′
bZIP28	5′-CATTTCCGCCACTTTTCAAT-3′	5′-TTCTAGCAGCAAACGGAGGT-3′
bZIP60	5′-ATCCGTCTCCTCCACTCCTT-3′	5′-GTCTTCGAGCTGCTTCTGCT-3′
ACTIN	5′-GCCGTACAACTGGTATTGTT-3′	5′-TCCAACTCCTGCTCATAATC-3′

not uniform for all root cells. Besides to dying cells, others still alive were also present, especially at treatments not exceeding 24 h (data not shown). Although the external cell layers, like root epidermis, seemed to be most affected, there was no indication for tissue- or cell-specific response to W treatment.

Subcellular effects of W in pea root cells

The cortical microtubule array is among the first subcellular components affected by W (Adamakis et al. 2010a). After 24 h of continuous W treatment, most pea root cells contained W-affected microtubules (W-microtubules, for

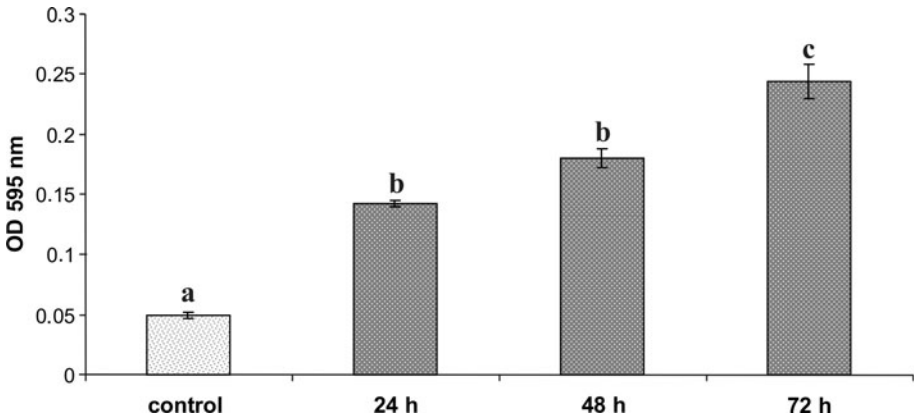

Fig. 1 Estimation of cell death rate in pea roots after W treatment by Evans Blue absorbance. Optical density (OD) of extracts from untreated roots (control) and roots treated with W for 24, 48 and 72 h, measured at 595 nm, increased gradually as W treatment was prolonged. *Values* correspond to mean ± SE of three independent experiments. *Different letters* represent statistically significant difference at $P < 0.05$

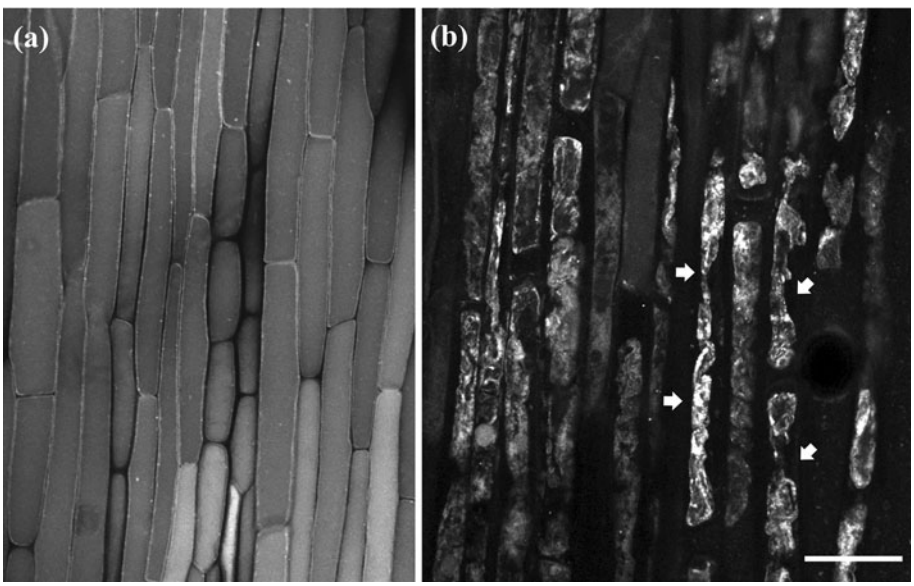

Fig. 2 FM4-64 fluorescence of untreated (**a**) and 24 h W-treated (**b**) root epidermal cells of pea. Extensive protoplast shrinkage (*arrows* in **b**), as expressed by plasma membrane detachment from the cell wall, can be observed after W treatment, unlike the uniform fluorescence and smooth outline of the untreated cells (**a**). *Bar* 20 μm

brevity). The cortical W-microtubules were fewer, shorter and disoriented (Fig. 3b), in contrast to the uniformly arranged, regularly oriented microtubules of untreated cells (Fig. 3a). Besides disruption of the cortical microtubules, almost no dividing cells could be observed after 24 h of W treatment. Among the extremely scarce (1–2 in each root cell population) mitotic cells, abnormal prophase cells without perinuclear microtubules (Fig. 3d; cf. c) and cells with atypical metaphase spindles (Fig. 3f; cf. e) were encountered. In addition, F-actin was also affected by W. After 24 h of W treatment, the root epidermal cells exhibited disrupted actin filaments, in comparison with those of untreated roots (Fig. 4b; cf. a).

Following disruption of the cytoskeleton, the nuclei of W-affected cells exhibited aberrant morphology, revealed by both propidium iodide staining and TEM. Defects in the nucleus were visible after 24 h of continuous W exposure. In all cells with affected nucleus W-microtubules were observed. While the nuclei of untreated root cells had normal appearance with evenly distributed chromatin (Fig. 5a, b), the nuclei of W-affected root cells exhibited condensed chromatin, which was distributed mainly at the periphery of the nucleus (Fig. 5c, d). In some cases, the dense peripheral chromatin appeared enclosed in double membranes, resembling the nuclear envelope (Fig. 6), like intranuclear mini-nuclei (Fig. 6; see also Online Resource, Fig. 1). Multi-lobed nuclei were frequent (Online Resource, Fig. 1), while in nuclei with condensed and peripherally distributed chromatin, entrapments of cytoplasmic components (ribosomes, mitochondria,

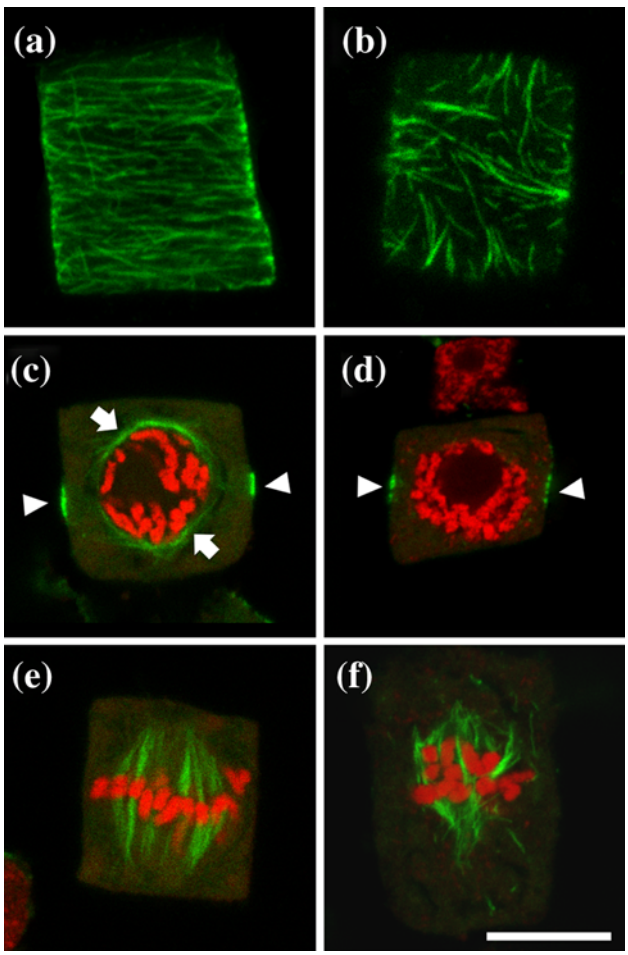

Fig. 3 Tubulin immunostaining (**a**–**f**) and DNA staining (**c**–**f**) of untreated (**a**, **c**, **e**) and W-treated (**b**, **d**, **f**) pea root cells. **a**, **b** Interphase cells: typical cortical microtubules exist in the untreated cell (**a**), while those of the W-treated cell are few, short and disoriented, exhibiting V-like convergence points (**b**). **c**, **d** Preprophase cells: while preprophase microtubule band (*arrowheads*) is visible in both untreated (**c**) and W-treated (**d**), perinuclear preprophase microtubules like those of the untreated cell (*arrows* in **c**) cannot be observed in the W-treated one (**d**). Note that, according to chromatin condensation, both preprophase cells are at a similar stage. **e**, **f** Metaphase cells: the spindle of W-treated cell is distorted (**f**), unlike the typical one of the untreated cell (**e**). *Bar* 10 μm

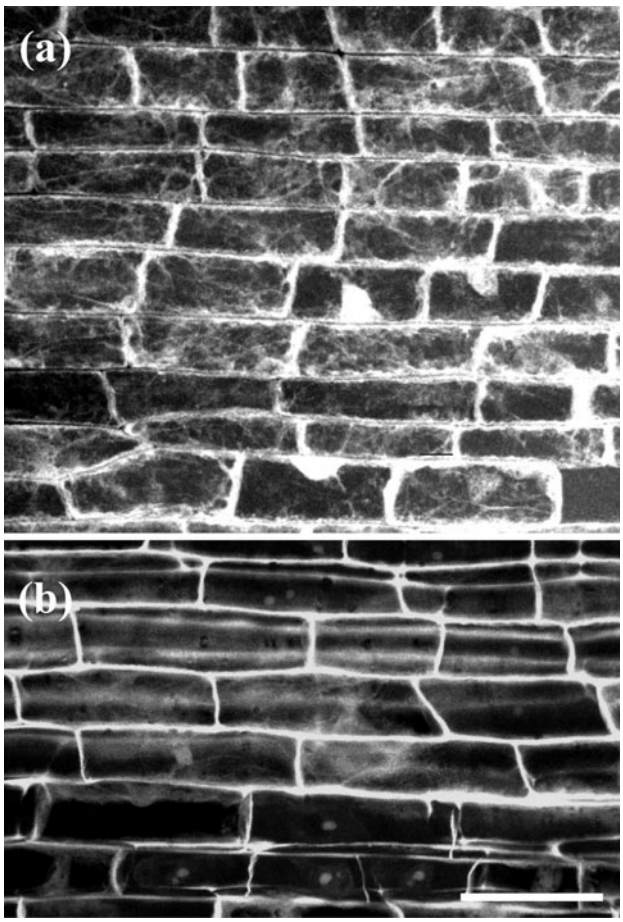

Fig. 4 Images of F-actin, after TRITC-phalloidin staining, in untreated (**a**) and W-treated (**b**) root epidermal cells. Both images are projections of 30 CLSM sections. Note the almost total disruption of actin filaments in W-treated cells (**b**), as compared with the prominent F-actin network of untreated cells (**a**). *Bar* 20 μm

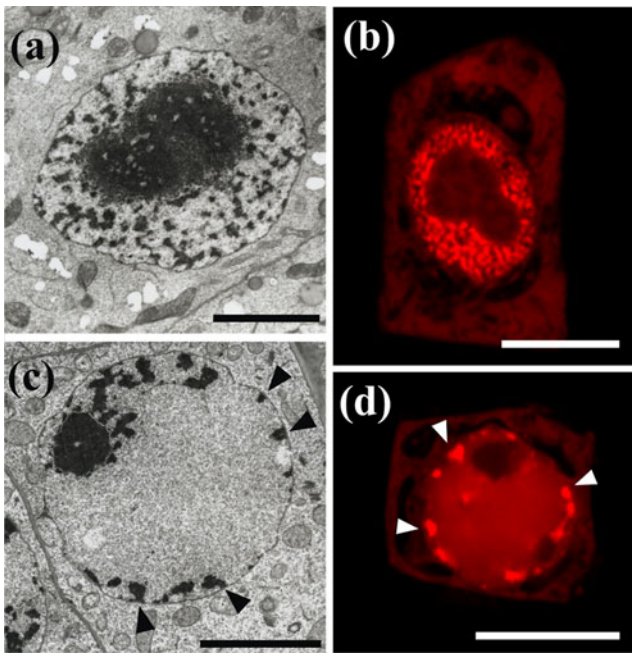

Fig. 5 TEM micrographs (**a**, **c**) and CLSM images after DNA staining with propidium iodide (**b**, **d**), illustrating the nuclei of untreated (**a**, **b**) and W-treated (**c**, **d**) meristematic root cells. Even distribution of chromatin can be observed in the nuclei of untreated cells (**a**, **b**). In the nuclei of W-treated cells the chromatin is condensed and distributed peripherally, just beneath the nuclear envelope (*arrowheads* in **c**, **d**). *Bars* 5 μm for **a** and **c**, 10 μm for **b** and **d**

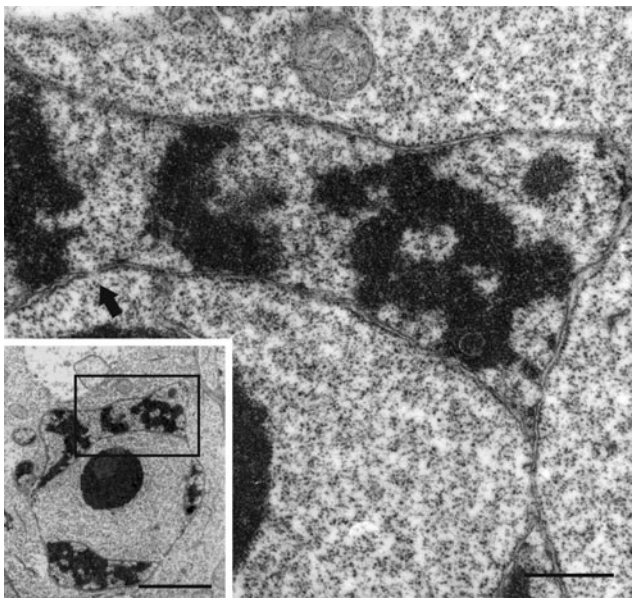

Fig. 6 TEM micrograph illustrating a nucleus with condensed chromatin, confined in peripheral intranuclear membrane compartments (*inset*) and an intranuclear membrane compartment of the above nucleus (defined by *rectangle* in the *inset*) at higher magnification. Double membrane surrounds a peripheral intranuclear chromatin group. Note that pores are present on the internal double membrane (*arrow*), which is coated with ribosomes. *Bars* 1, 5 μm for *inset*

membranes, vacuoles and lipid bodies) were also encountered (Online Resource, Fig. 1).

Detection of DNA fragmentation and gene expression

In order to observe whether W induced DNA laddering, a typical hallmark of PCD (review by Lam et al. 1999), DNA isolated from roots either untreated or treated with W for 24, 48 and 72 h was subjected to 2% agar electrophoresis. DNA obtained from roots treated with W for 24 and 48 h appeared as a single high molecular weight band (data not shown). After 72 h of treatment, no sign of DNA laddering could be observed but slight smearing was detectable (Fig. 7a). Even in prolonged W treatments (5 days), DNA smearing was not increased and DNA laddering was not observed (data not shown).

To confirm, at the molecular level, the view that W might induce PCD, we examined the effect of W on the expression of two specific plant genes, *HSR203J*, an early marker of hypersensitive response-PCD (Pontier et al. 1998), and the plant homolog of *DAD-1* (Orzáez and Granell 1997). *HSR203J* was not detectably expressed in untreated roots (Fig. 7b). Mild *HSR203J* expression was found after 12 h of W treatment, which was pronounced after 24 h of W treatment (Fig. 7b). After 12 h of W treatment, the expression of *DAD-1* was enhanced, while it was silenced after 24 h of treatment (Fig. 7b).

To further assess the possible correlation of W-effect with ER stress and UPR, we also examined the expression of *BiP-D* (Noh et al. 2003; Kamauchi et al. 2005; Urade 2009), *bZIP28* (Liu et al. 2007; Tajima et al. 2008; Oono et al. 2010) and *bZIP60* (Iwata and Koizumi 2005a; Iwata et al. 2008; Lu and Christopher 2008; Tajima et al. 2008) in W-treated pea roots. *BiP-D* expression was elevated after 12 h of treatment, while it was decreased at 24 h, still being higher than before treatment (Fig. 7c). The expression of *bZIP28* and *bZIP60* also increased after 12 and 24 h of W treatment (Fig. 7d, e).

Treatment with 26S proteasome and caspase inhibitors

The participation of the 26S proteasome and caspase pathways in the W-effect was examined indirectly by treating pea seedlings with combinations of the relevant inhibitors (MG132 and Z-VAD-FMK, respectively) and W.

Initially, the possible effect of these inhibitors on cortical microtubule organization, nucleus morphology and cell division in root tip cells was examined by 24 h treatment with the inhibitors alone. In general, the above features in inhibitor-treated cells were indistinguishable from those of untreated cells. The effects of these inhibitors on cortical microtubules, the nucleus and cell cycle progression were negligible (Online Resource, Fig. 2).

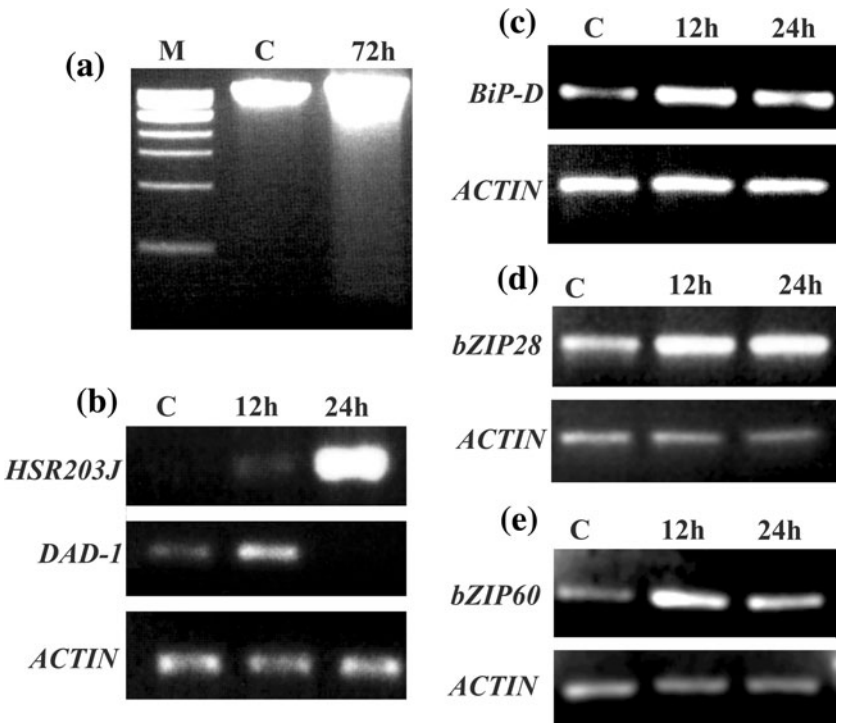

Fig. 7 **a** Genomic DNA fragmentation in roots either untreated (*C*) or treated for 72 h with W (*72 h*). Lane (*M*) is a standard molecular weight marker. Slight DNA smearing can be observed after 72 h of W treatment, indicating degradation but not laddering. **b** Expression profile of *HSR203J* and *DAD-1* genes in roots either untreated (*C*) or treated with W for 12 h (*12 h*) and 24 h (*24 h*). *HSR203J* was not detectably expressed in untreated roots. Its expression was mild after 12 h and pronounced after 24 h of treatment. After 12 h of W treatment, the expression of *DAD-1* was enhanced, while it was silenced after 24 h. **c** Expression of *BiP-D* in roots either untreated (*C*) or treated with W for 12 h (*12 h*) and 24 h (*24 h*). *BiP-D* expression was elevated after 12 h of treatment and it lowered at 24 h, still being higher than that of untreated roots. **d** Expression of *bZIP28* in roots either untreated (*C*) or treated with W for 12 h (*12 h*) and 24 h (*24 h*). *bZIP28* expression was elevated after 12 h and 24 h of treatment. **e** Expression of *bZIP60* in roots either untreated (*C*) or treated with W for 12 h (*12 h*) and 24 h (*24 h*). Like *bZIP28*, the expression of *bZIP60* was elevated after 12 and 24 h of treatment. *ACTIN* expression was used as control for cDNA amount and quality for **b**–**e**

Accordingly, study with combined treatments of the inhibitors with W was performed as follows.

In seedlings pre-treated with 100 μM MG132 for 24 h and then treated for 24 h with 200 mg/L W + 100 μM MG132, interphase root tip cells displayed cortical microtubule organization (Figs. 8a; cf. 3a) and nuclear morphology (Figs. 8b; cf. 5b) similar to that of untreated cells, while dividing cells were abundant (Fig. 8c, d). The results were similar in seedlings pre-treated with 100 μM Z-VAD-FMK for 24 h and then transferred for 24 h to 200 mg/L W + 100 μM Z-VAD-FMK (Figs. 8e, f; cf. 3a, 5b; 8g, h). In the above treatment combinations, Evans Blue absorbance appeared reduced compared with that detected after exposure to W alone for 24 h (Fig. 9). These combined treatments (inhibitors → tungsten + inhibitors) also alleviated the effect of W on the expression profile of *DAD-1*, *HSR203J*, *BiP-D*, *bZIP28* and *bZIP60*. After such treatments, in which MG132 and Z-VAD-FMK were combined with W, expression of *DAD-1* gene was still observable (though lower than that of untreated material), no expression of *HSR203J* was noticed and the expression levels of *BIP-D*, *bZIP28* and *bZIP60* appeared reduced compared to those in roots treated with W alone (Online Resource, Fig. 3).

When seedlings were treated directly for 24 h with 200 mg/L W + 100 μM MG132 solution, the root cells exhibited normal appearance (typical cortical microtubule organization, regular nucleus morphology and abundant dividing cells; Online Resource, Fig. 4). However, in seedlings treated directly for 24 h with 200 mg/L W + 100 μM Z-VAD-FMK, root cells were similar to those treated with W alone (Online Resource, Fig. 5; cf. Fig. 3b).

PBA treatment

To further examine whether ER stress is involved in W-induced PCD, some pea seedlings were treated with a PBA + W combination. The appearance of the cortical microtubules, the nucleus and cell cycle phases of cells treated with PBA alone, was similar to that of untreated cells (Online Resource, Fig. 6). In seedlings treated

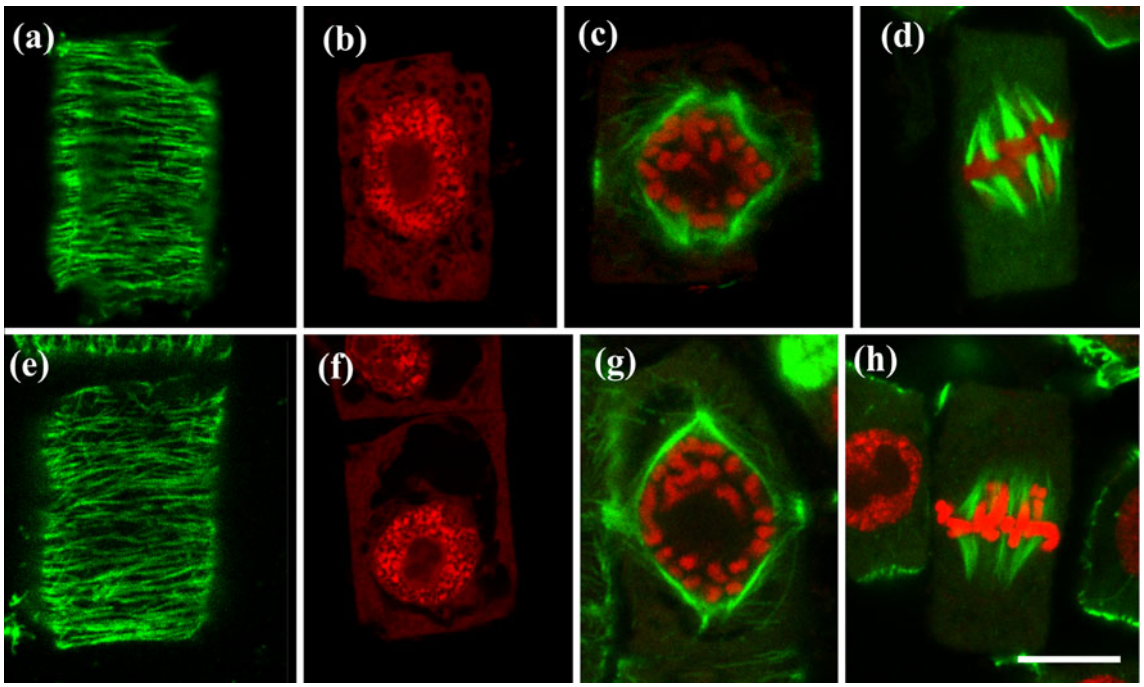

Fig. 8 Tubulin immunostaining (**a, c–e, g, h**) and DNA staining (**b–d**, **f–h**) in root cells treated with combinations of MG132 (**a–d**) or Z-VAD-FMK (**e–h**) and W. Interphase cells, pretreated for 24 h with MG132 or Z-VAD-FMK and then treated for another 24 h with the above inhibitors + W, exhibit typical cortical microtubules (**a**, **e**), similar to those of untreated cells (cf. Fig. 3a). The nuclei of cells treated in the above way exhibit normal chromatin configuration (**b**, **f**) comparable to that of untreated cells (cf. Fig. 5b). Typical prophase (**c**, **g**) and metaphase (**d**, **h**) cells were present in roots treated with the above combinations. *Bar* 10 μm

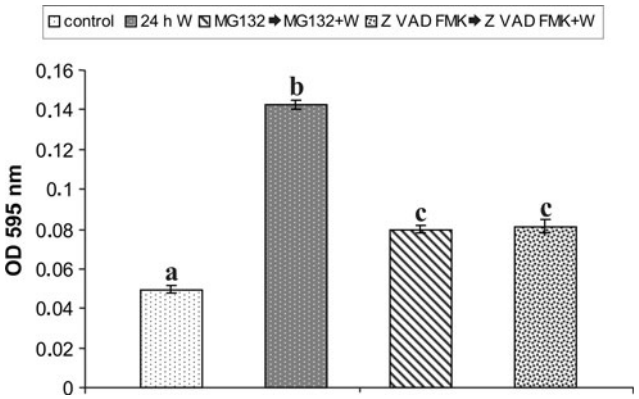

Fig. 9 The optical density (OD) at 595 nm of pea root extracts, after Evans Blue staining and extraction. Extracts derived from untreated roots (control), W-treated roots (24 h W), roots pre-treated with MG132 for 24 h followed by treatment with MG132 + W for another 24 h (MG132 → MG132 + W), and roots pre-treated with Z-VAD-FMK for 24 h followed by 24 h treatment with Z-VAD-FMK + W (Z-VAD-FMK → Z-VAD-FMK + W). The extract OD after the last two treatments is higher than that of the extract of untreated roots, yet lower than that of the extract of roots treated with W alone. *Values* correspond to mean ± SE of three independent experiments. *Different letters* represent statistically significant difference at $P < 0.05$

directly with 200 mg/L W + 250 μM PBA for 24 h, root tip cells displayed cortical microtubule organization and nucleus appearance similar to that of untreated cells (Fig. 10a, b) with abundant dividing cells (Fig. 10a, b). Moreover, after the above treatment, Evans Blue absorbance appeared reduced in comparison to that detected in treatments with W alone for 24 h (Fig. 10c). In roots treated with PBA + W, *DAD-1* was still expressed, while expression of the *HSR203J* was not detected (Online Resource, Fig. 3). The mRNA levels of *BiP-D*, *bZIP28* and *bZIP60* genes were also reduced in roots treated with PBA + W, as opposed to those in roots subjected to W alone (Online Resource, Fig. 3).

Discussion

W induces PCD in *Pisum sativum* root

As already shown, W is fatal for the main root of *Pisum sativum* (Adamakis et al. 2008). The root is a plant organ consisting of heterogeneous tissues and cell types, from small meristematic cells to long vacuolated ones, arranged in several cell files and layers. These cells respond differently to abiotic stimuli, according to their identity (Dinneny et al. 2008). Thus, the morphological manifestation of the effects of W is expected not to be uniform among the whole cell population of even a single pea root.

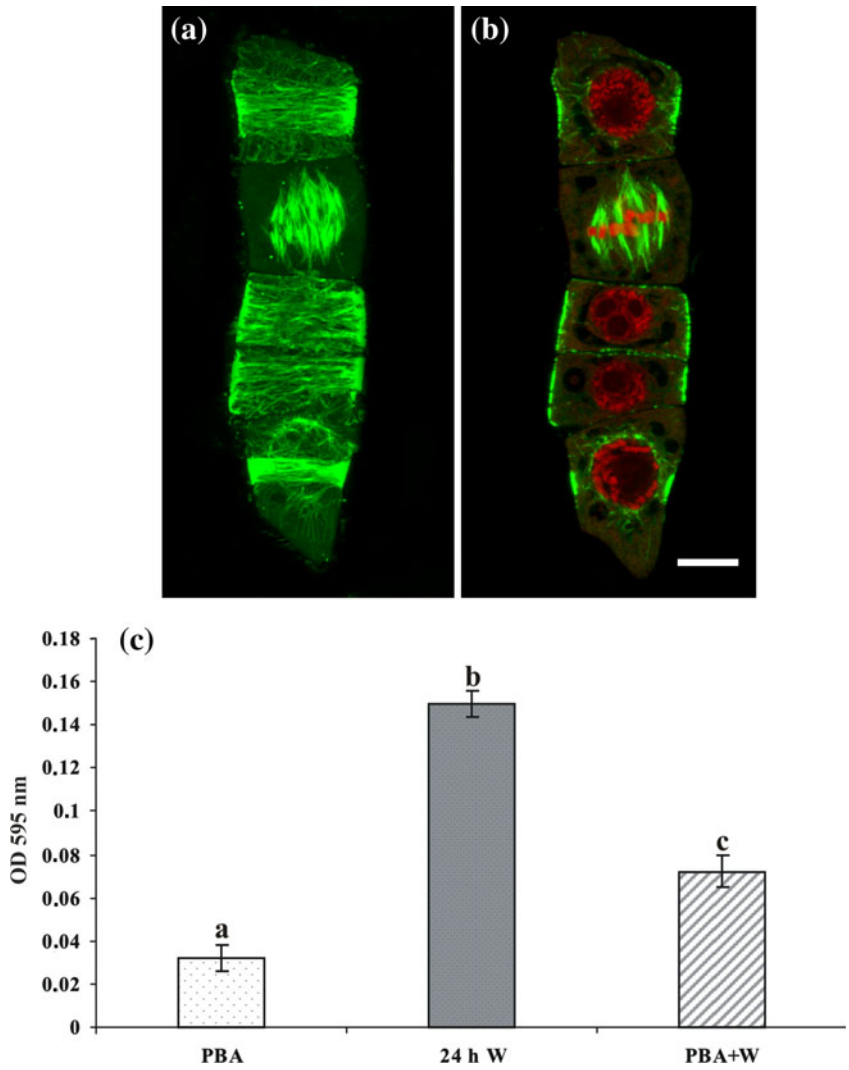

Fig. 10 Tubulin immunostaining (**a**) and DNA staining (**b**) in root cells treated with PBA + W for 24 h. **a**, **b** Single CLSM sections through the cortical and central plane, respectively, of the same cells. Interphase cells exhibit typical cortical microtubules (**a**), similar to those of untreated cells (cf. Fig. 3a). Their nuclei exhibit normal chromatin configuration (**b**) comparable to that of untreated cells (cf. Fig. 5b). Typical preprophase and metaphase cells were present (**a**, **b**; cf. Fig. 3c, e, respectively) in roots treated with the above combinations. *Bar* 10 μm. **c** Diagram depicting the optical density (OD) at 595 nm of pea root extracts, after Evans Blue staining and extraction. Extracts derived from PBA-treated roots, W-treated roots (24 h W) and roots treated with a PBA + W combination for 24 h. The extract OD after the last treatment is higher than that of roots treated with PBA, however significantly lower than that of roots treated with W alone. *Bars* represent the standard error. *Values* correspond to mean ± SE of three independent experiments. *Different letters* represent statistically significant difference at $P < 0.05$

The main features of W toxicity in pea root cells were: (a) increase of Evans Blue absorbance, which was enhanced in prolonged treatments (Fig. 1), (b) retraction of the plasma membrane from the cell wall and shrinkage of the protoplast (Fig. 2b), (c) disruption of cortical microtubules (Fig. 3b; see also Adamakis et al. 2010a) and F-actin cytoskeleton (Fig. 4b), (d) arrest of cell divisions, chromatin condensation and peripheral distribution in the nucleus (Fig. 5c, d). In addition, the expression levels of *DAD-1*, *HSR203J*, *BiP-D, bZIP28* and *bZIP60* genes were modified (Fig. 7b–e).

Several of the features mentioned previously, such as chromatin condensation, protoplast shrinkage and increase of Evans Blue absorbance are typical of plant PCD (Danon et al. 2004; review by Reape et al. 2008). Moreover, the data concerning *DAD1* and *HSR203J* expression profiles strongly support that W induces PCD in *Pisum sativum* root (see "Introduction"). Disruption of the cytoskeleton appears to be a general trait of heavy metal toxicity (Přibyl et al. 2008; Dho et al. 2010 and references therein). In particular, the cortical microtubules are shown to be a widespread target of W among land plants (Adamakis et al. 2010b). Accordingly, in this study, we considered cortical microtubule appearance as a reliable indicator of W toxicity.

The fact that inhibition of the 26S proteasome and caspase pathways in W-treated roots rescues cortical microtubules, diminishes Evans Blue absorbance, restores expression of *DAD-1* and abolishes *HSR203J* expression, as compared with roots treated with W alone, provides further evidence that some kind of PCD occurs in root cells as a response to W treatment (Suarez et al. 2004; Zuppini et al. 2004; Vacca et al. 2007). PCD in the main root may be a necessary "sacrifice", some kind of "amputation", in order to protect the rest of the plant from being contaminated with W. Indeed, it has been shown that while the main root is affected by W, as assessed by microtubule disruption, the leaves do not exhibit any visible disturbance (Adamakis et al. 2010b). Besides, in response to W toxicity lateral roots emerge (Adamakis et al. 2008; see also Xiong

et al. 2009). As the main root dies, effort is probably put on penetrating into W-free soil by lateral roots. The characteristics and peculiarities of W-induced PCD (W-PCD for brevity) are discussed below.

Pea roots under W-PCD: monitoring of dying cells

Arrest of cell division is common in cells that execute PCD (review by Lam et al. 1999). In the meristematic cells of *Pisum sativum* root, this may explain the multi-lobed appearance of several nuclei and the presence of cytoplasm and organelles entrapped inside the nucleoplasm. As is the case for cells treated with anti-mitotic drugs (among others see Karagiannidou et al. 1995), because of microtubule disruption due to W, new nuclear envelopes surround unsegregated chromosome groups, resulting in polyploid multi-lobed nuclei. During this process, accidental entrapment of cytoplasmic components inside the nucleus may also occur.

The distribution and condensation of chromatin in W-affected cells is typical of PCD, while DNA laddering is a hallmark of the majority but not of all the cases of cells that execute PCD (review by Reape et al. 2008). According to our observations, it seems that W-PCD might not comprise the latter feature. Instead, DNA smearing was detected in roots treated with W for 72 h (Fig. 7a). Neither DNA laddering nor an increase in DNA smearing was observed even in W treatments up to 5 days (data not shown). Similar observations were made in several other cases of PCD, e.g. during lace plant leaf development (Gunawardena et al. 2004; Lord and Gunawardena 2011) and water stress in *Arabidopsis thaliana* (Duan et al. 2010). The fact that DNA smearing in our study was not extensive can be attributed to the complexity of the root. As previously mentioned, cells were not uniformly affected by W and, as a result, cells with PCD features may reside in the vicinity of cells still alive even in the same root.

Although typical caspases have not been found in plants, proteases with similar activity, named caspase-like proteases or metacaspases, participate in plant PCD (review by Bonneau et al. 2008). Recently, a common substrate of caspases and metacaspases has been identified (Sundström et al. 2009). Caspase inhibitors have been successfully used to prevent the action of the above enzymes (reviews by Rotari et al. 2005; Bonneau et al. 2008). In particular, Z-VAD-FMK, a pan-caspase inhibitor, has been applied to prevent various kinds of PCD in plant cells (Elbaz et al. 2002; Mlejnek and Procházka 2002). In the present study, Z-VAD-FMK rescued the cortical microtubules, diminished Evans Blue intake, restored expression of *DAD-1* and abolished the expression of *HSR203J*, in comparison with roots treated with W alone. It can therefore be assumed that caspase-like proteases might participate in W-PCD.

The role of the 26S proteasome in PCD is undoubtedly a matter of controversy. In contrast to the "mainstream" opinion that inhibition of 26S proteasome activity accelerates PCD (among others see Grimm and Osborne 1999; Kim et al. 2003), several authors have claimed that 26S proteasome inhibition prevents or delays PCD (Vacca et al. 2007; Valenti et al. 2008; He and Kermode 2010; this study).

As previously shown in animal and yeast cells (Kisselev et al. 2003), apart from ubiquitin-related protein degradation, 26S proteasome also exhibits some caspase-like activity. Recently, this was shown also for the 26S proteasome in plants. In particular, Hatsugai et al. (2009) found that 26S proteasome might exert a caspase3 function and it can be inhibited by both a 26S proteasome inhibitor and a caspase3 inhibitor. It could therefore be concluded that treatment with MG132 results also in inhibition of any caspase-like activity of the 26S proteasome. This may well explain our observation that inhibition of the 26S proteasome prevents W-PCD, as manifested by microtubule organization, progression of cell division, Evans Blue intake and *DAD-1* and *HSR203J* expression profiles.

According to our results, MG132 can inhibit the effect of W by both pre-treatment and simultaneous combined treatment with W. On the contrary, Z-VAD-FMK inhibited the effect of W only with pre-treatment. It can be therefore assumed that 26S proteasome activity participates at a rather late stage of PCD cascade, while the caspase-like proteases that are inhibited by Z-VAD-FMK are activated earlier than the 26S proteasome.

W-PCD seems to be induced by ER stress-UPR

The question that emerges is how W-PCD is triggered. As discussed below, several data of this study support that ER stress may be implicated in the induction of W-PCD. ER stress was found to be associated with apoptosis in animal cells (Boyce and Yuan 2006). In plants, ER stress as a PCD-triggering pathway is also currently under consideration (Cacas 2010; Duan et al. 2010). Several of the findings of this study, such as modification of *DAD-1* expression, imply that W-PCD may occur through the above pathway. *DAD-1* is involved in the avoidance of PCD (Tanaka et al. 1997; Danon et al. 2004) and its expression is reduced or totally silenced during various PCD programs (van der Kop et al. 2003; Yamada et al. 2004).

In *Pisum sativum* roots treated with W for 12 h, *DAD-1* is overexpressed denoting some "self-defense" effort; after 24 h of continuous W treatment, attenuation and complete silencing of *DAD-1* implies that root cells ultimately "surrender" and undergo W-PCD (Fig. 7b). *DAD-1* encodes a subunit of oligosaccharyltransferase, which

participates in N-linked protein glycosylation in the ER, a post-transcriptional modification fundamental for proper protein folding (Lindholm et al. 2000; review by Schröder and Kaufman 2005). Inhibition of N-linked protein glycosylation results in accumulation of unfolded proteins in the ER lumen, initiating the UPR, which, in turn, triggers PCD (reviews by Urade 2009; Cacas 2010). As *DAD-1* is silenced in W-treated pea root, oligosaccharyltransferase activity may be compromised, resulting in a failure of N-linked protein glycosylation. This may initiate UPR and, by domino effect, activate caspase-like proteases that prompt W-PCD.

Elevated *BiP-D*, *bZIP28,* and *bZIP60* expression, as well as induction of *HSR203J* expression, further support the above view. *BiP-D* expression remains low during normal conditions but it can increase under UPR. It encodes the luminal binding protein which is ER-located and specifically binds to the unfolded proteins (among others see Noh et al. 2003; Kamauchi et al. 2005; Urade 2009). As a consequence, its expression increase is used as marker of UPR in eukaryotic cells. bZIP28 is a membrane-tethered transcription factor, implicated in the regulation of UPR-stress-related genes (Liu et al. 2007). In short tunicamycin treatments (up to 4 h) the expression of *bZIP28* was not upregulated (Liu et al. 2007). However, a mild induction of bZIP28 transcripts was shown in *Arabidopsis thaliana* seedlings treated with tunicamycin for 5 and 10 h and in rice endosperm cells accumulating β-amyloid peptide (Tajima et al. 2008; Oono et al. 2010). In the present study, W treatment was applied for 24 h. Therefore, it seems that elevated *bZIP28* expression might be necessary for the execution of W-induced UPR during such a long treatment. What is more, *bZIP60* expression was elevated during W treatment, which has generally been found to occur during treatments with ER stress-inducing factors (see Iwata et al. 2008; Lu and Christopher 2008; Tajima et al. 2008; Oono et al. 2010). bZIP60 is a membrane-associated transcription factor and its expression was found to be specific for ER stress, since it has been found to be specifically induced in treatments with another ER-inducing agent, DTT (Oono et al. 2010). Hence, elevated *bZIP60* expression, in combination with the elevated expression of *bZIP28* and *BiP-D*, could indicate the execution of W-induced ER stress-UPR response. *HSR203J* was originally isolated from tobacco as a hypersensitive response-PCD-associated gene (Pontier et al. 1998). *HSR203J* homologs have also been found in other plant species (see Pontier et al. 2004), and its expression is generally considered as a marker for PCD. In addition, *HSR203J* and *BiP-D* expression has been shown to be stimulated after experimental inhibition of N-linked protein glycosylation by tunicamycin (Iwata and Koizumi 2005b), correlating UPR with PCD. Importantly, in the latter experiments as well as the present study, *HSR203J* expression peaks at 24 h of treatment. Taking into account all the above, it could be assumed that W-PCD may occur as a result of UPR, due to silencing of *DAD-1* after treatment with W.

Indirect evidence derived from PBA + W treatment further supports the above view. PBA is commonly used as a therapeutic agent against pathologic ER stress-resulting neurological diseases (see Wiley et al. 2010 and references therein). Apart from this, it has been used to rescue plants from ER stress-derived PCD. It has been shown that sodium 4-phenylbutyrate (an other aromatic derivative of butyric acid), chemically supporting ER protein folding, alleviated PCD features of *Arabidopsis thaliana* cells treated with an inducer of ER stress (Watanabe and Lam 2008). Roots of *Pisum sativum* seedlings subjected to PBA + W treatment exhibited low levels of *BiP-D*, *bZIP28* and *bZIP60* expression (Online Resource, Fig. 3), reduced Evans Blue intake, microtubule integrity and cell cycle progression (Fig. 10), unlike those treated with W alone (cf. Fig. 3b, d, f). Accordingly, it seems that PBA "rescued" *Pisum sativum* root cells from the toxic effect of W.

The fact that combined treatments with W and the 26S proteasome inhibitor reduced the expression of *BiP-D*, *bZIP28* and *bZIP60* deserves further attention. In yeast and animal cells, ER-associated degradation (ERAD) of misfolded proteins is accomplished by the ubiquitin/26S proteasome system and, therefore, inhibition of the latter results in an enhancement of UPR (see review by Urade 2007 and references therein). In plants, however, ERAD is also accomplished by an ubiquitin/26S proteasome-independent pathway, the molecular mechanism of which remains unknown, as discussed by Urade (2007). In accordance, inhibition of the 26S proteasome by MG132 may not prevent ERAD in plant cells, which seems to be the case for W-affected *Pisum sativum* root cells. Instead of hindering ERAD, MG132 seems to be mainly responsible for the inhibition of the already mentioned caspase3-like activity of the 26S proteasome (Hatsugai et al. 2009), thus preventing PCD. The reduced expression of *BiP-D*, *bZIP28* and *bZIP60*, obtained by combined treatments with W and the pan-caspase inhibitor, are also in accordance with the above view. Taken together, these data indicate that as W toxicity is exerted the expression of these UPR-related genes is associated with the activity of caspase-like proteases.

Concluding remarks and perspectives

In conclusion, PCD in W-affected *Pisum sativum* roots seems to occur by ER stress-UPR. Cacas (2010) has raised the questions: "…which abiotic/biotic stresses and developmental signals can induce ER stress? Is ER stress

encountered in specific PCD forms?" Water stress has been recently shown to induce PCD by the ER stress pathway (Duan et al. 2010). According to our study, W toxicity seems to be another abiotic factor that induces PCD by the ER stress-UPR pathway. The fact that W may induce PCD further supports the toxic character of W for plants as a pollutant. More questions arise however. How does W affect *DAD-1* expression to induce UPR? It has been proposed that W enters plant cells by binding to Cnx1 protein (Adamakis et al. 2010a). What may be the relation of this binding to PCD induction? Further experimentation is needed to provide the appropriate answers.

Acknowledgments We are grateful to Dr. Dimitra Papaefthimiou, Institute of Agrobiotechnology, CERTH, Thessaloniki, for assistance with primer designing and helpful suggestions concerning the PCR experiments. Dr. Anastasia Tsingotjidou, Faculty of Veterinary Medicine of Aristotle University, cordially provided access to the Nikon D-Eclipse C1 CLSM. We also thank the anonymous reviewers for their constructive suggestions and comments.

Conflict of interest The authors declare that they have no conflict of interest.

References

Adamakis I-DS, Eleftheriou EP, Rost TL (2008) Effects of sodium tungstate on the ultrastructure and growth of pea (*Pisum sativum*) and cotton (*Gossypium hirsutum*) seedlings. Environ Exp Bot 63:416–425

Adamakis I-DS, Panteris E, Eleftheriou EP (2010a) Tungsten affects the cortical microtubules of *Pisum sativum* root cells: Experiments on tungsten-molybdenum antagonism. Plant Biol 12:114–124

Adamakis I-DS, Panteris E, Eleftheriou EP (2010b) The cortical microtubules are a universal target of tungsten toxicity among land plant taxa. J Biol Res 13:59–66

Bézier A, Lambert B, Baillieul F (2002) Study of defense-related gene expression in grapevine leaves infected with *Botrytis cinerea*. Eur J Plant Pathol 108:111–120

Bonneau L, Ge Y, Drury GE, Gallois P (2008) What happened to plant caspases? J Exp Bot 59:491–499

Bosch M, Franklin-Tong VE (2007) Temporal and spatial activation of caspase-like enzymes induced by self-incompatibility in *Papaver* pollen. Proc Natl Acad Sci USA 104:18327–18332

Bosch M, Poulter NS, Vatovec S, Franklin-Tong VE (2008) Initiation of programmed cell death in self-incompatibility: role for cytoskeleton modifications and several caspase-like activities. Mol Plant 1:879–887

Boyce M, Yuan J (2006) Cellular response to endoplasmic reticulum stress: a matter of life or death. Cell Death Differ 13:363–373

Cacas JL (2010) Devil inside: does plant programmed cell death involve the endomembrane system? Plant Cell Environ 33:1453–1473

Cascardo JC, Almeida RS, Buzeli RA, Carolino SM, Otoni WC, Fontes EP (2000) The phosphorylation state and expression of soybean BiP isoforms are differentially regulated following abiotic stresses. J Biol Chem 275:14494–14500

Chen PY, Lee KT, Chi WC, Hirt H, Chang CC, Huang HJ (2008) Possible involvement of MAP kinase pathways in acquired metal-tolerance induced by heat in plants. Planta 228:499–509

Clausen JL, Korte N (2009) Environmental fate of tungsten from military use. Sci Total Environ 407:2887–2893

Danon A, Rotari VI, Gordon A, Mailhac N, Gallois P (2004) Ultraviolet-C overexposure induces programmed cell death in *Arabidopsis*, which is mediated by caspase-like activities and which can be suppressed by caspase inhibitors, p35 and defender against apoptotic death. J Biol Chem 279:779–787

Dho S, Camusso W, Mucciarelli M, Fusconi A (2010) Arsenate toxicity on the apices of *Pisum sativum* L. seedling roots: effects on mitotic activity, chromatin integrity and microtubules. Environ Exp Bot 69:17–23

Dinneny JR, Long TA, Wang JY, Mace D, Pointer S, Barron C, Brady SM, Schiefelbein J, Benfey PN (2008) Cell identity mediates the response of *Arabidopsis* roots to abiotic stress. Science 32:942–945

Duan Y, Zhang W, Li B, Wang Y, Li K, Sodmergen, Han C, Zhang Y, Li X (2010) An endoplasmic reticulum response pathway mediates programmed cell death of root tip induced by water stress in *Arabidopsis*. New Phytol 186:681–695

Elbaz M, Avni A, Weil M (2002) Constitutive caspase-like machinery executes programmed cell death in plant cells. Cell Death Differ 9:726–733

Grimm LM, Osborne BA (1999) Apoptosis and the proteasome. Results Probl Cell Differ 23:209–228

Gunawardena AHLAN, Greenwood JS, Dengler NG (2004) Programmed cell death remodels lace plant leaf shape during development. Plant Cell 16:60–73

Hatsugai N, Iwasaki S, Tamura K, Kondo M, Fuji K, Ogasawara K, Nishimura M, Nishimura IH (2009) A novel membrane fusion-mediated plant immunity against bacterial pathogens. Genes Dev 23:2496–2506

He X, Kermode AR (2010) Programmed cell death of the megagametophyte during post-germinative growth of white spruce (*Picea glauca*) seeds is regulated by reactive oxygen species and the ubiquitin-mediated proteolytic system. Plant Cell Physiol 51:1707–1720

Iakimova ET, Woltering EJ, Kapchina-Toteva VM, Harren FJM, Cristescu SM (2008) Cadmium toxicity in cultured tomato cells—role of ethylene, proteases and oxidative stress in cell death signaling. Cell Biol Int 32:1521–1529

Iwata Y, Koizumi N (2005a) An *Arabidopsis* transcription factor, AtbZIP60, regulates the endoplasmic reticulum stress response in a manner unique to plants. Proc Natl Acad Sci USA 102: 5280–5285

Iwata Y, Koizumi N (2005b) Unfolded protein response followed by induction of cell death in cultured tobacco cells treated with tunicamycin. Planta 220:804–807

Iwata Y, Fedoroff NV, Koizumi N (2008) *Arabidopsis* bZIP60 is a proteolysis-activated transcription factor involved in the endoplasmic reticulum stress response. Plant Cell 20:3107–3121

Kamauchi S, Nakatani H, Nakano C, Urade R (2005) Gene expression in response to endoplasmic reticulum stress in *Arabidopsis thaliana*. FEBS J 272:3461–3476

Karagiannidou T, Eleftheriou EP, Tsekos I, Galatis B, Apostolakos P (1995) Colchicine-induced paracrystals in root cells of wheat (*Triticum aestivum* L.). Ann Bot 76:23–30

Kim M, Ahn JW, Jin UH, Choi D, Paek KH, Pai HS (2003) Activation of the programmed cell death pathway by inhibition of proteasome function in plants. J Biol Chem 278:19406–19415

Kisselev AF, Garcia-Calvo M, Overkleeft HS, Peterson E, Pennington MW, Ploegh HL, Thornberry NA, Goldberg AL (2003) The caspase-like sites of proteasomes, their substrate specificity, new

inhibitors and substrates, and allosteric interactions with the trypsin-like sites. J Biol Chem 278:35869–35877
Koutsospyros A, Braida W, Christodoulatos C, Dermatas D, Strigul N (2006) A review of tungsten: from environmental obscurity to scrutiny. J Hazard Mater 136:1–19
Kuthanova A, Fischer L, Nick P, Opatrny Z (2008) Cell cycle phase-specific death response of tobacco BY-2 cell line to cadmium treatment. Plant Cell Environ 31:1634–1643
Lam E, Pontier D, del Pozo O (1999) Die and let live - programmed cell death in plants. Curr Opin Plant Biol 2:502–507
Liao Y, Zou HF, Wei W, Hao YJ, Tian AG, Huang J, Liu YF, Zhang JS, Chen SY (2008) Soybean GmbZIP44, GmbZIP62 and GmbZIP78 genes function as negative regulator of ABA signaling and confer salt and freezing tolerance in transgenic Arabidopsis. Planta 228:225–240
Lindholm P, Kuittinen T, Sorri O, Guo D, Merits A, Tormakangas K, Runeberg-Roos P (2000) Glycosylation of phytepsin and expression of dad1, dad2 and ost1 during onset of cell death in germinating barley scutellum. Mech Dev 93:169–173
Liu JX, Srivastava R, Che P, Howell SH (2007) An endoplasmic reticulum stress response in *Arabidopsis* is mediated by proteolytic processing and nuclear relocation of a membrane associated transcription factor, bZIP28. Plant Cell 19:4111–4119
Lord CEN, Gunawardena AHLAN (2011) Environmentally induced programmed cell death in leaf protoplasts of *Aponogeton madagascariensis.* Planta 233:407–421
Lu DP, Christopher DA (2008) Endoplasmic reticulum stress activates the expression of a sub-group of protein disulfide isomerase genes and AtbZIP60 modulates the response in *Arabidopsis thaliana*. Mol Genet Genomics 280:199–210
Mlejnek P, Procházka S (2002) Activation of caspase-like proteases and induction of apoptosis by isopentenyladenosine in tobacco BY-2 cells. Planta 215:158–166
Noh SJ, Kwon CS, Oh DH, Moon JS, Chung WI (2003) Expression of an evolutionarily distinct novel *BiP-D* gene during the unfolded protein response in *Arabidopsis thaliana*. Gene 311:81–91
Oono Y, Wakasa Y, Hirose S, Yang L, Sakuta C, Takaiwa F (2010) Analysis of ER stress in developing rice endosperm accumulating β-amyloid peptide. Plant Biotechnol J 8:691–718
Orzáez D, Granell A (1997) The plant homologue of the defender against apoptotic death gene is down-regulated during senescence of flower petals. FEBS Lett 404:275–278
Osterburg AR, Robinson CT, Schwemberger S, Mokashi V, Stockelman M, Babcock GF (2010) Sodium tungstate (Na_2WO_4) exposure increases apoptosis in human peripheral blood lymphocytes. J Immunotoxicol 7:174–182
Pan JW, Zhu MY, Chen H (2001) Aluminum-induced cell death in root-tip cells of barley. Environ Exp Bot 46:71–79
Panteris E, Galatis B, Quader H, Apostolakos P (2007) Cortical actin filament organization in developing and functioning stomatal complexes of *Zea mays* and *Triticum* turgidum. Cell Motil Cytoskelet 64:531–548
Pontier D, Tronchet M, Rogowsky P, Lam E, Roby D (1998) Activation of hsr203j, a plant gene expressed during incompatible plant-pathogen interactions, is correlated with programmed cell death. Mol Plant Microbe Interact 11:544–554
Pontier D, del Poso O, Lam E (2004) Cell death in plant disease: mechanisms and molecular markers. In: Nooden LD (ed) Plant cell death processes. Elsevier Academic Press, San Diego, pp 37–50
Poulter NS, Vatovec S, Franklin-Tong VE (2008) Microtubules are a target for self-incompatibility signaling in *Papaver* pollen. Plant Physiol 146:1358–1367
Přibyl P, Cepák V, Zachleder V (2008) Cytoskeletal alterations in interphase cells of the green alga *Spirogyra decimina* in response to heavy metals exposure: II. The effect of aluminium, nickel and copper. Toxicol In Vitro 22:1160–1168
Reape TJ, Molony EM, McCabe PF (2008) Programmed cell death in plants: distinguishing between different modes. J Exp Bot 59:435–444
Rotari VI, He R, Gallois P (2005) Death by proteases in plants: whodunit. Physiol Plant 123:376–385
Schröder M, Kaufman RJ (2005) ER stress and the unfolded protein response. Mutat Res 569:29–63
Steinberg KK, Relling MV, Gallagher ML, Greene CN, Rubin CS, French D, Holmes AK, Carroll WL, Koontz DA, Sampson EJ, Satten GA (2007) Genetic studies of a cluster of acute lymphoblastic leukaemia cases in Churchill County, Nevada. Environ Health Persp 115:158–164
Suarez MF, Filonova LH, Smertenko A, Savenkov EI, Clapham DH, von Arnold S, Zhivotovsky B, Bozhkov PV (2004) Metacaspase-dependent programmed cell death is essential for plant embryogenesis. Curr Biol 14:R339–R340
Sundström JF, Vaculova A, Smertenko AP, Savenkov EI, Golovko A, Minina E, Tiwari BS, Rodriguez-Nieto S, Zamyatnin AA, Välineva T, Saarikettu J, Frilander MJ, Suarez MF, Zavialov A, Ståhl U, Hussey PJ, Silvennionen O, Sundberg E, Zhivotovsky B, Bozhkov PV (2009) Tudor staphylococcal nuclease is an evolutionarily conserved component of the programmed cell death degradome. Nat Cell Biol 11:1347–1354
Tajima H, Iwata Y, Iwano M, Takayama S, Koizumi N (2008) Identification of an *Arabidopsis* transmembrane bZIP transcription factor involved in the endoplasmic reticulum stress response. Biochem Biophys Res Commun 374:242–247
Tamas L, Budikova S, Huttova J, Mistrik I, Simonovicova M, Siroka B (2005) Aluminium-induced cell death of barley-root border cells is correlated with peroxidase- and oxalate oxidase-mediated hydrogen peroxide production. Plant Cell Rep 24:189–194
Tanaka Y, Makishima T, Sasabe M, Ichinose Y, Shiraishi T, Nishimoto T, Yamada T (1997) DAD-1**,** a putative programmed cell death suppressor gene in rice. Plant Cell Physiol 38:379–383
Urade R (2007) Cellular response to unfolded proteins in the endoplasmic reticulum of plants. FEBS J 274:1152–1171
Urade R (2009) The endoplasmic reticulum stress signalling pathways in plants. BioFactors 35:326–331
Vacca RA, Valenti D, Bobba A, de Pinto MC, Merafina RS, De Gara L, Passarella S, Marra E (2007) Proteasome function is required for activation of programmed cell death in heat shocked tobacco Bright-Yellow 2 cells. FEBS Lett 581:917–922
Valenti D, Vacca RA, Guaragnella N, Passarella S, Marra E, Giannattasio S (2008) A transient proteasome activation is needed for acetic acid-induced programmed cell death to occur in *Saccharomyces cerevisiae*. FEMS Yeast Res 8:400–404
van der Kop DAM, Ruys G, Dees D, van der Schoot C, de Boer AD, van Doorn WG (2003) Expression of defender against apoptotic death (DAD-1) in *Iris* and *Dianthus* petals. Physiol Plant 117: 256–263
Watanabe N, Lam E (2008) BAX inhibitor-1 modulates endoplasmic reticulum stress-mediated programmed cell death in *Arabidopsis*. J Biol Chem 238:3200–3210
Wiley JC, Meabon JS, Frankowski H, Smith EA, Schecterson LC, Bothwell M, Ladiges WC (2010) Phenylbutyric acid rescues endoplasmic reticulum stress-induced suppression of APP proteolysis and prevents apoptosis in neuronal cells. PlosONE 5:e9135
Wilson B, Pyatt FB (2006) Bio-availability of tungsten in the vicinity of an abandoned mine in the English Lake District and some potential health implications. Sci Total Environ 370:401–408
Xiong J, Lu H, Lu K, Duan Y, Zhu C (2009) Cadmium decreases crown root number by decreasing endogenous nitric oxide,

which is indispensable for crown root primordia initiation in rice seedlings. Planta 230:599–610

Yamada T, Takatsu Y, Kasumi M, Marubashi W, Ichimura K (2004) A homolog of the defender against apoptotic death gene (DAD1) in senescing gladiolus petals is down-regulated prior to the onset of programmed cell death. J Plant Physiol 161:1281–1283

Zuppini A, Navazio L, Mariani P (2004) Endoplasmic reticulum stress-induced programmed cell death in soybean cells. J Cell Sci 117:2591–2598